

Mamatkodiurov B.D., Yakubov.Y.Y.,

Mukhammadaliev Kh.G., Serobov A.N.

*Institute of General and Inorganic Chemistry of Uzbekistan Academy of Sciences, 100170, Mirzo
Ulug'bek str., 77a. Uzbekistan.*

Orunbaev Khalmyrat, Orunbaev H.G.

*Director of the Laboratory of Nanotechnology of the Technology Center of the Academy of Sciences
of Turkmenistan. Turkmenistan.*

Samandarov E. Sh., Kodamboev P. K.,

Khorezm Mamun branch of Uzbekistan Academy of Sciences, Markaz-1, Khiva 220900, Uzbekistan.

ADSORPTION PROPERTIES OF CARBON NANOTUBE BASED ON CYCLOPENTADIENYL IRON DICARBONYL DIMER

Abstract: In this study, the adsorption capacity of single-walled carbon nanotubes (CNTs based on cyclopentadienyl iron dicarbonyl dimer) arrays towards pure N₂ gas was investigated experimentally and computationally at 77 K and in the pressure range from 0.01 to 1 atm. The experimental work represents gravimetric surface excess adsorption measurements of each gas studied on this nanomaterial. Commercial samples of CNTs based on pure CNTs, which were systematically prepared and initially characterized, were used to evaluate their adsorption capacity. The BET (Brunauer-Emmett-Teller) equation was adopted to estimate the overall adsorption isotherm based on the experimental surface excess adsorption data for each studied system.

Key word: Carbon nanotubes; morphologies; Cyclopentadienyliron dicarbonyl dimer [CpFe(CO)₂]₂; mesoporous; macropores; adsorption-desorption; Brunauer-Emmett-Teller .

Introduction.

Global warming and its consequences are compelling humanity to take serious measures. Emissions of gases such as nitrogen and carbon oxides are harmful to the environment and health. Simultaneously, the increasing energy demand and depletion of fossil fuel reserves necessitate the development of new energy strategies. The utilization of physical and chemical adsorption on solid sorbents in H₂ and other gas storage technologies is an effective method. The sorbent must possess properties such as high adsorption capacity, chemical stability, low cost, and lightness. For instance, porous materials with a high surface area are advantageous for the efficient storage of H₂. Carbon nanotubes (CNTs) are acknowledged as promising materials for H₂ storage, CO₂ capture, and the separation of gas mixtures. Conversely, the rapid growth of energy demand and the gradual depletion of fossil fuel reserves underscore the need for the development of new strategies for energy source production and utilization of their energy content.

Cyclopentadienyliron dicarbonyl dimer is an organometallic compound with the formula [(η⁵-C₅H₅)Fe(CO)₂]₂, often abbreviated to Cp₂Fe₂(CO)₄, [CpFe(CO)₂]₂ or even Fp₂, with the colloquial name "fip dimer". It is a dark reddish-purple crystalline solid, which is readily soluble in moderately polar organic solvents such as chloroform and pyridine, but less soluble in carbon

tetrachloride and carbon disulfide. $\text{Cp}_2\text{Fe}_2(\text{CO})_4$ is insoluble in but stable toward water. $\text{Cp}_2\text{Fe}_2(\text{CO})_4$ is reasonably stable to storage under air and serves as a convenient starting material for accessing other Fp ($\text{CpFe}(\text{CO})_2$) derivatives (described below).

Discussion and Results.

The investigation and characterization of nitrogen adsorption represent a dynamic area of scientific inquiry. This holds particular significance for the advancement of novel materials with enhanced properties. Characteristics such as surface area, porosity, and pore size serve as pivotal factors in molding the functional attributes of materials. They exert a significant influence on adsorption capacity, activity, and stability[1].

Utilizing the Quantachrome® ASiQwin™- Automated Gas Sorption version 5.21 device, we conducted a study on carbon nanotubes synthesized based on cyclopentadienyl iron dicarbonyl dimer. (Table 1-2)

Analysis		Report	
Operator	1	File name	Carbon nanotube
Date	20.09.2024	Instrument	Autosorb iQ Station 2
Sample Weight	0.0173 g	Outgas Temp	120 °C
Outgas Time	1.0 hrs	Non-ideality	6.58e-05 1/Torr
Analysis gas	Nitrogen	Bath temp	77.35 K
Analysis Time	3:14 hr:min	Cold Zone V	1.73258 cc
Analysis Mode	Standard	CellType	9mm w/o rod
VoidVol. Mode	He Measure	Warm Zone V	15.1206 cc

(Table -1)

ANALYSIS		Report	
OPERATOR	1	File name	Nanotruba-2.qps
DATE	20.09.2024	Instrument	Autosorb iQ Station 2
SAMPLE WEIGHT	0.003 g	Outgas Temp	120 °C
OUTGAS TIME	1.0 hrs	Non-ideality	6.58e-05 1/Torr
ANALYSIS GAS	Nitrogen	Bath temp	77.35 K
ANALYSIS TIME	3:09 hr:min	Cold Zone V	1.73454cc
ANALYSIS MODE	Standard	CellType	9mm w/o rod

VOIDVOL. MODE	He Measure	Warm Zone V	16.6087 cc
----------------------	------------	-------------	------------

(Table -2)

Accordingly, the nitrogen adsorption characteristics of carbon nanotubes based on cyclopentadienyl iron dicarbonyl dimer are disclosed. The analysis reveals a substantial potential for nitrogen adsorption. Furthermore, it was observed that the resultant carbon nanotube-1 possesses a BET (Brunauer-Emmett-Teller) surface area of 65.9558 m²/g, an average pore diameter of 6.259 Å, and an adsorption volume of 1.632 cm³/g. Conversely, Nanotube-2 exhibits a BET surface area of 357.0415 m²/g, an average pore diameter of 0.697 Å, and an adsorption volume of 6.933 cm³/g. The elimination of additives from the nanotube composition evidently led to a substantial increase in both the surface area and adsorption volume of the nanotubes. Tables 1-2-3 and Figures 1-2 provide essential parameters such as surface area, pore size, and their size distribution. These parameters were determined utilizing the appropriate adsorption isotherm models.

At relative pressure (P/P ₀ =0-0.02)	Carbon nanotube-1	Carbon nanotube-2
S _{BET} , m ² /g	65.9558	357.0415
t-Plot Micropore Area, m ² /g	56.1923	143.7773
t-Plot external surface area, m ² /g	101.9197	390.5442
Cumulative surface area of mesopores (BJH), m ² /g	103.6722	452.6063
t-Plot micropore volume, cm ³ /g	1.632	6.933
Mesopores cumulative volume, cm ³ /g	0.010320	0.006223
Maximum pore volume (HK), cm ³ /g	0.016347	0.028494
Average pore diameter (4V/A by BET), Å	6.259 Å	0.697 Å
Median pore width, Å	14.401	17.250
Average pore hydraulic radius (V/A by MP method), Å	10.1093 Å	10.5225

(Table -3)

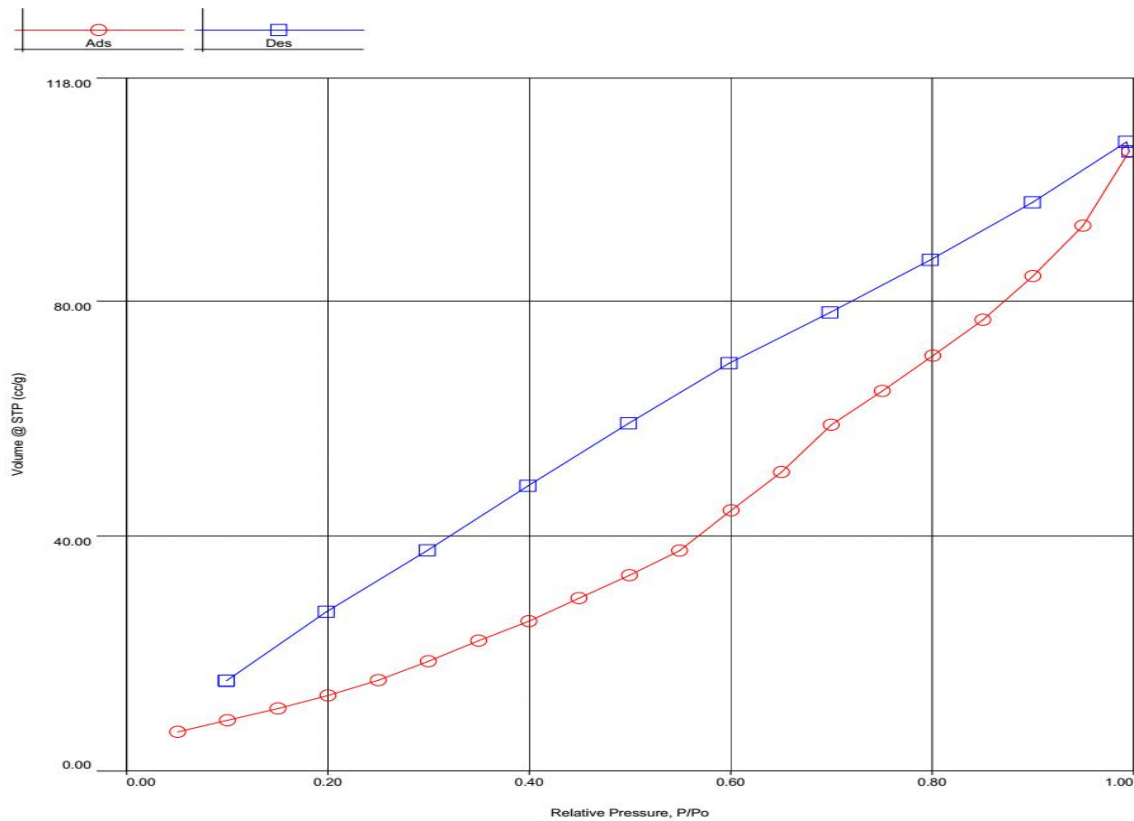


Figure -1.

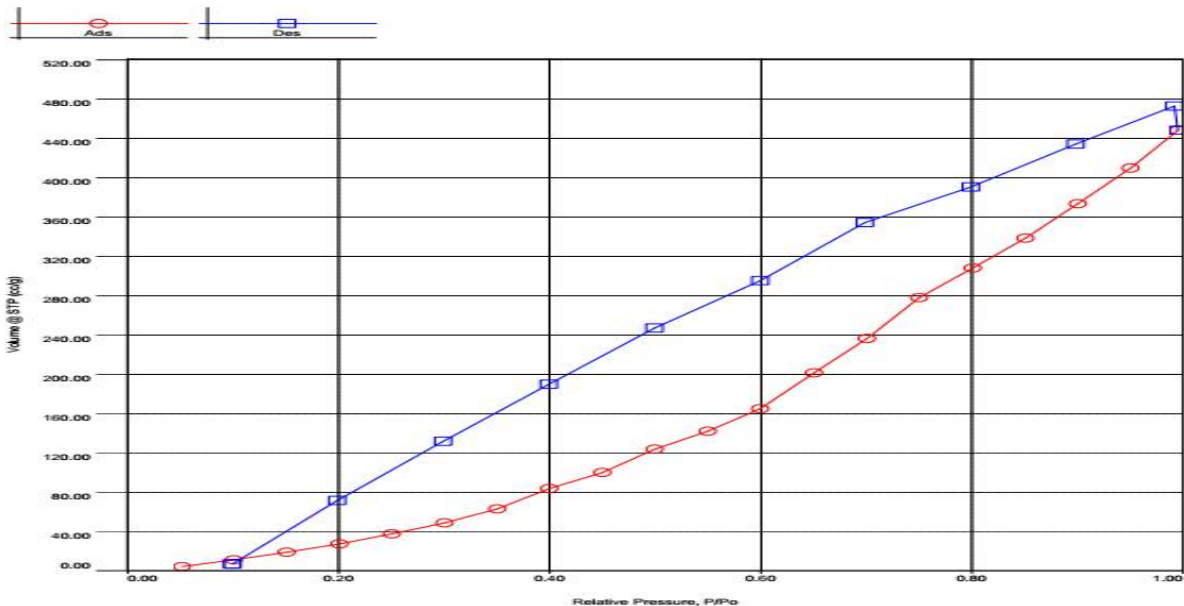


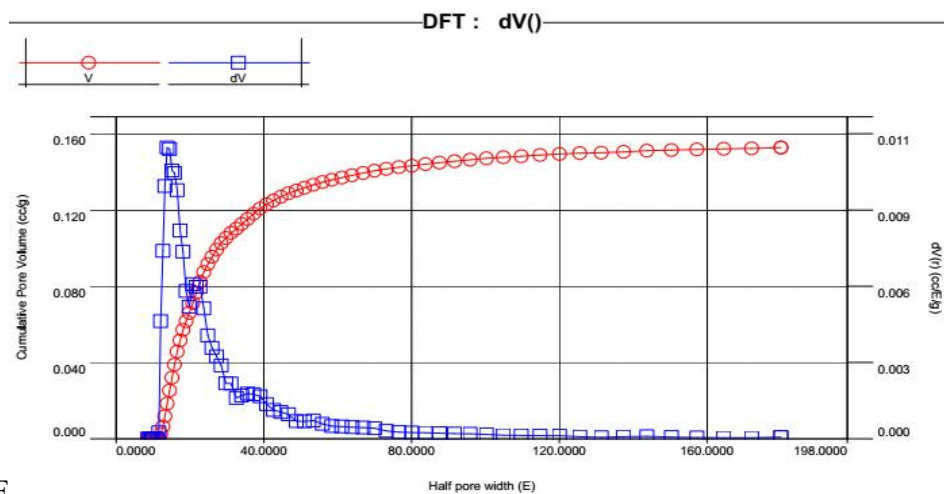
Figura- 2.

The shape of the isotherm indicates a type IV classification, suggesting a mesoporous structure. This type of isotherm is particularly suitable for materials undergoing capillary condensation. The upward trend of the isotherm curves at higher relative pressures signifies the existence of large macropores within the structure. Describing the adsorption mechanism in porous materials becomes

feasible through this analysis. Additionally, the presence of hysteresis is noted in the nanotube isotherm (Figure 1-2). While various forms of hysteresis loops have been documented, the primary types, namely H1, H2, H3, H4, and H5 as listed by IUPAC [2], correspond to the H3 type of hysteresis observed in the isotherm curves displayed in Figure 1-2. This particular type, although uncommon, features open and partially obstructed mesopores with a distinct shape associated with certain porous structures [3]. Initially, within the isotherm curve ($p/p_0 \sim 0.4 - 0.5$ for nitrogen at 77 K), a linear nitrogen absorption increase is evident, signifying the saturation of the microporous structure [4].

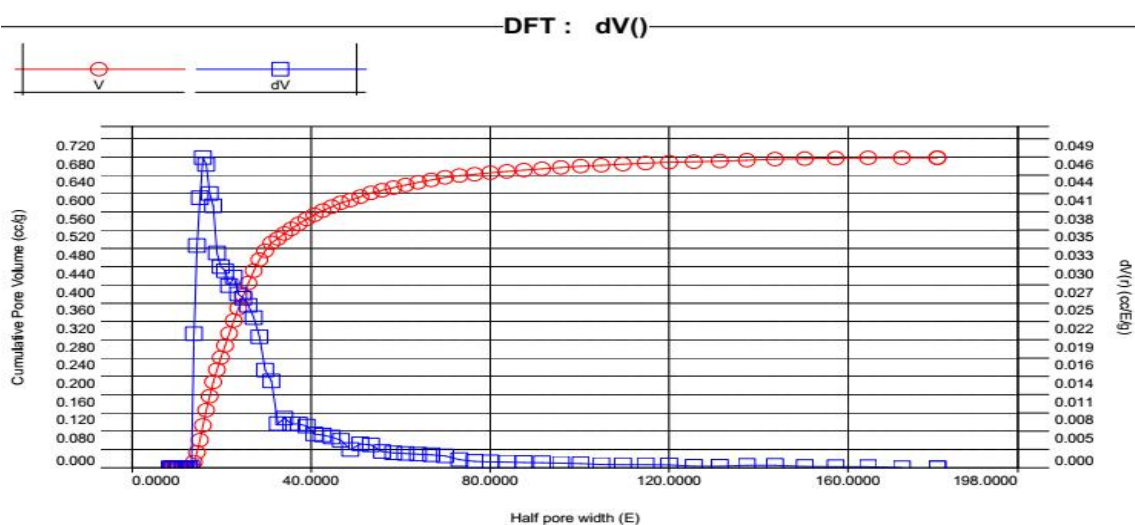
The nitrogen adsorption rises as the relative pressure nears $p/p_0 \sim 1$, indicating capillary condensation in meso- and macropores. The steep ascent in these curves points towards the presence of significant pores [5].

Consequently, the adsorption-desorption curves for carbon nanotubes synthesized based on Cyclopentadienyl iron dicarbonyl dimer reveal heterogeneous N_2 adsorption characteristics in the structure, showcasing the existence of meso- and macropores.



(F)

3-rasm



4-rasm

Conclusion.

The analysis revealed that the synthesized Nanotube-1 exhibited a BET (Brunauer-Emmett-Teller) surface area of 65.9558 m²/g, an average pore diameter of 6.259 Å, and an adsorption volume of 1.632 cm³/g. Following treatment of the nanotubes with a mild acid solution at varying temperatures, Nanotube-2 displayed a BET surface area of 357.0415 m²/g, an average pore diameter of 0.697 Å, and an adsorption volume of 6.933 cm³/g. It is evident that the elimination of metal compounds obstructing gas absorption in the mesopores resulted in a reduction in the average pore diameter. Moreover, the removal of additives from the nanotubes led to a substantial increase in both the surface area and adsorption volume of the nanotubes.

Furthermore, the adsorption-desorption curves illustrated the heterogeneous N₂ adsorption structural characteristics of carbon nanotubes fabricated based on Cyclopentadienyl iron dicarbonyl dimer, showcasing the presence of meso- and macropores.

References:

1. S. Kitagawa, R. Kitaura, S. Noro, Functional Porous Coordination Polymers, *Angew Chem Int Ed* 43 (2004) 2334–2375. <https://doi.org/10.1002/anie.200300610>.
2. X.-L. Qi, J.-W. Ye, R.-B. Lin, P.-Q. Liao, S.-Y. Liu, C.-T. He, J.-P. Zhang, X.-M. Chen, Syntheses, structures and gas sorption properties of two coordination polymers with a unique type of supramolecular isomerism, *Inorg. Chem. Front.* 2 (2015) 136–140. <https://doi.org/10.1039/C4QI00190G>.
3. B. Moulton, M.J. Zaworotko, From Molecules to Crystal Engineering: Supramolecular Isomerism and Polymorphism in Network Solids, *Chem. Rev.* 101 (2001) 1629–1658. <https://doi.org/10.1021/cr9900432>.
4. E.R. Engel, J.L. Scott, Advances in the green chemistry of coordination polymer materials, *Green Chem.* 22 (2020) 3693–3715. <https://doi.org/10.1039/D0GC01074J>.
5. S.R. Batten, N.R. Champness, X.-M. Chen, J. Garcia-Martinez, S. Kitagawa, L. Öhrström, M. O’Keeffe, M. Paik Suh, J. Reedijk, Terminology of metal–organic frameworks and coordination polymers (IUPAC Recommendations 2013), *Pure and Applied Chemistry* 85 (2013) 1715–1724. <https://doi.org/10.1351/PAC-REC-12-11-20>.
6. Y. Wang, D. Astruc, A.S. Abd-El-Aziz, Metallopolymers for advanced sustainable applications, *Chem. Soc. Rev.* 48 (2019) 558–636. <https://doi.org/10.1039/C7CS00656J>.
7. A.K. Cheetham, C.N.R. Rao, R.K. Feller, Structural diversity and chemical trends in hybrid inorganic–organic framework materials, *Chem. Commun.* (2006) 4780–4795. <https://doi.org/10.1039/B610264F>.
8. K. Biradha, A. Ramanan, J.J. Vittal, Coordination Polymers Versus Metal–Organic Frameworks, *Crystal Growth & Design* 9 (2009) 2969–2970. <https://doi.org/10.1021/cg801381p>.
9. J. Liu, H. Yu, L. Wang, Z. Deng, K.-R. Naveed, A. Nazir, F. Haq, Two-dimensional metal–organic frameworks nanosheets: Synthesis strategies and applications, *Inorganica Chimica Acta* 483 (2018) 550–564. <https://doi.org/10.1016/j.ica.2018.09.011>.
10. M. Zhao, Q. Lu, Q. Ma, H. Zhang, Two-Dimensional Metal–Organic Framework Nanosheets, *Small Methods* 1 (2017) 1600030. <https://doi.org/10.1002/smt.201600030>.
11. C. Tan, X. Cao, X.-J. Wu, Q. He, J. Yang, X. Zhang, J. Chen, W. Zhao, S. Han, G.-H. Nam, M. Sindoro, H. Zhang, Recent Advances in Ultrathin Two-Dimensional Nanomaterials, *Chem. Rev.* 117 (2017) 6225–6331. <https://doi.org/10.1021/acs.chemrev.6b00558>.

12. W. Xia, J. Li, T. Wang, L. Song, H. Guo, H. Gong, C. Jiang, B. Gao, J. He, The synergistic effect of Ceria and Co in N-doped leaf-like carbon nanosheets derived from a 2D MOF and their enhanced performance in the oxygen reduction reaction, *Chem. Commun.* 54 (2018) 1623–1626. <https://doi.org/10.1039/C7CC09212A>.
13. K. Zhao, S. Liu, G. Ye, Q. Gan, Z. Zhou, Z. He, High-yield bottom-up synthesis of 2D metal–organic frameworks and their derived ultrathin carbon nanosheets for energy storage, *J. Mater. Chem. A* 6 (2018) 2166–2175. <https://doi.org/10.1039/C7TA06916B>.
14. Z. Kang, L. Fan, D. Sun, Recent advances and challenges of metal–organic framework membranes for gas separation, *J. Mater. Chem. A* 5 (2017) 10073–10091. <https://doi.org/10.1039/C7TA01142C>.
15. A. Bétard, R.A. Fischer, Metal–Organic Framework Thin Films: From Fundamentals to Applications., *Chem. Rev.* 112 (2012) 1055–1083. <https://doi.org/10.1021/cr200167v>.
16. L. Tom, M.R.P. Kurup, A 2D-layered Cd(II) MOF as an efficient heterogeneous catalyst for the Knoevenagel reaction, *Journal of Solid State Chemistry* 294 (2021) 121846. <https://doi.org/10.1016/j.jssc.2020.121846>.
17. P. Li, W. Liu, J.S. Dennis, H.C. Zeng, Ultrafine Alloy Nanoparticles Converted from 2D Intercalated Coordination Polymers for Catalytic Application, *Adv Funct Materials* 26 (2016) 5658–5668. <https://doi.org/10.1002/adfm.201601174>.
18. A.M. Kirillov, Y.Y. Karabach, M.V. Kirillova, M. Haukka, A.J.L. Pombeiro, Topologically Unique 2D Heterometallic Cu^{II}/Mg Coordination Polymer: Synthesis, Structural Features, and Catalytic Use in Alkane Hydrocarboxylation, *Crystal Growth & Design* 12 (2012) 1069–1074. <https://doi.org/10.1021/cg201459k>.
19. S. Zhou, G. Yan, B. Gao, W. Jiang, B. Liu, T. Zhou, C. Liu, G. Che, A layered Mn-based coordination polymer as an efficient heterogeneous catalyst for CO₂ cycloaddition under mild conditions, *CrystEngComm* 24 (2022) 4527–4533. <https://doi.org/10.1039/D2CE00579D>.
20. X.-K. Yang, M.-N. Chang, J.-F. Hsing, M.-L. Wu, C.-T. Yang, C.-H. Hsu, J.-D. Chen, Synthesis, crystal structures and thermal properties of six Co(II) and Ni(II) coordination polymers with mixed ligands: Formation of a quadruple-strained helical nanotube, *Journal of Molecular Structure* 1171 (2018) 340–348. <https://doi.org/10.1016/j.molstruc.2018.06.036>.